Structure-properties relation for random networks of fibers with noncircular cross section

S. Deogekar and R. C. Picu

Phys. Rev. E **95**, 033001 — Published 1 March 2017

DOI: 10.1103/PhysRevE.95.033001

Structure-Properties Relation for Random Networks of Fibers with Non-Circular Cross-Section

S. Deogekar and R.C. Picu[1]

Department of Mechanical, Aerospace and Nuclear Engineering, Rensselaer Polytechnic Institute, Troy, NY 12180

Abstract

The mechanical behavior of 3D cross-linked random fiber networks composed from fibers of non-circular cross-section characterized by two principal moments of inertia is studied in this work. Such fibers store energy in the axial deformation mode and two bending modes of unequal stiffness. We show that the torsional stiffness of fibers becomes important as it determines the relative contribution of the two bending modes to the overall deformation. The scaling of the small strain modulus with the network parameters is established. The large strain deformation of these structures is less sensitive to the shape of the cross-section.

[1] Corresponding author: Tel: +1 518 276 2195, Fax: +1 518 276 6025, E-mail: picuc@rpi.edu (R.C. Picu)

1. Introduction

Various natural materials are made from fibers arranged randomly to form multifunctional and complex structures. Connective tissue is composed from collagen fibrils which bundle together to form fibers [1]. These are connected on larger scales either randomly, as in cartilage, or in even larger bundles, as in tendons. Fibrous networks are also a common occurrence in man-made materials such as felt, paper, textiles etc [2]. Nonwovens composed of entangled, slender fibers are used for thermal and acoustic insulation. They are also used for liquid absorption in hygiene products, hence finding application in personal care products, baby diapers etc. A special type of random fiber networks (Voronoi networks) is structurally similar to open-cell foams. These are used in packaging materials, automobile seats and as filters in air-conditioning systems [3]. In all these applications, fibers are too large to be affected by thermal fluctuations and hence these networks are athermal.

A fiber network can be described by a number of parameters important in the overall mechanical behavior of the material. The structure of the network is usually described by the network density, ρ, computed as the total fiber length per unit volume. If fibers are preferentially oriented, the orientation tensor can be also used as a structural descriptor. Other parameters, such as the spatial fluctuations of the density, orientation and cross-link density may be important, but are rarely considered when discussing the relationship between network structure and properties. In addition, the fibers properties are essential. These include the area, A, and the moments of inertia of the fiber cross-section. In random networks the fiber segment length (i.e. length of the segment between successive cross-links) is Poisson distributed and the mean of this distribution, l_c, is directly related to the network density, ρ, as $l_c \sim 1/D\rho$, where D is the fiber diameter [4]. The fiber slenderness is defined as $\sqrt{A}/l_c$.

In most studies to date all fibers in the network are considered of the same type [5,6,7,8,9] (networks made from dissimilar fibers are studied in [10]) and are, in general, of circular cross-section. However, many athermal fibers have non-circular sections which are characterized by two principal moments of inertia, I_{min} and I_{max}. Notoriously, the cellulose fibers of paper are ribbon-like [11]. If fibers can be considered beams, the polar moment of inertia, J, is given by J

$= I_{min} + I_{max}$. On the other hand, the effective axial, bending and torsional behaviors of molecular filaments (e.g. tropocollagen filaments large enough to behave athermally) are not controlled by the dimensions of the effective "filament cross-section", rather are defined by the intra-molecular interactions and by the size and position of the side groups which may lead to anisotropic behavior in the plane perpendicular to the filament axis.

These observations motivate the present study of athermal networks of fibers having non-circular section. We compare this class of materials with the more commonly studied networks of fibers with circular section and having same network architecture. For networks of cylindrical fibers, it has been established that the key parameters are the network density, ρ, and a parameter with units of length, $l_b = \sqrt{E_f I / E_f A}$, where E_f is the fiber material elastic modulus [5,7,8]. Parameter l_b indicates the relative importance of the bending and axial deformation modes of fibers in the overall mechanics of the network. For large ρ and l_b values, the network deformation is close to affine (local strains are identical to the far field applied strains) and the majority of the strain energy is stored in the axial deformation mode of fibers. When these parameters have small values, the deformation is non-affine and the energy is stored in the bending deformation mode. Hence, the network stores energy in the softest available deformation mode [5,7]. Consequently, the effective modulus of the network, *E*, is proportional to $E_f A$ in the affine regime and to $E_f I$ in the non-affine regime. In the affine regime $E \sim \rho$, while in the non-affine regime $E \sim \rho^x$, where the exponent *x* depends on the network architecture and embedding space dimensionality and takes values from 2 [12] to 8 [5,7,8]. Open cell foams have a similar behavior, with *x* = 2 in the non-affine regime [13]. Furthermore, it has been established that the torsional rigidity of fibers of circular section, which is proportional to *J*, is not of central importance, as the network of such fibers does not store much energy in the torsional mode for any range of the network parameters. This implies that *E* is not a function of *J* in any deformation regime.

If the fiber cross-section is not circular, the existence of two principal moments of inertia, I_{min} and I_{max}, indicates that bending can take place in either a softer or a stiffer mode. Two limits of the problem can be identified. Denote by l_b^t the value of parameter l_b which corresponds to the

transition from the bending dominated to the axial dominated deformation of the network for given density. If $l_{b\,min} = \sqrt{E_f I_{min}/E_f A} > l_b^t$, the bending stiffness of fibers is less important and the affine deformation regime is recovered. If $l_{b\,max} = \sqrt{E_f I_{max}/E_f A} < l_b^t$, the axial mode is less important and the non-affine regime described above is recovered. In this case, if the fibers were free to twist, the behavior would be controlled by $E_f I_{min}$ and the discussion would be identical to that of fibers with circular section and with $l_b = l_{b\,min} = \sqrt{E_f I_{min}/E_f A}$. However, fibers have a non-zero torsional stiffness which prevents them from rotating freely to enable the softest bending mode. Therefore, for the more interesting range $l_{b\,min} \leq l_b^t \leq l_{b\,max}$, parameter $G_f J$, which is proportional to the torsional stiffness, should matter. In this work we identify the effect of these parameters on the small strain modulus of the network, *E*, and on the large deformation tensile behavior.

2. Model and simulation details

Three types of three-dimensional networks, Voronoi, diluted Voronoi and Delaunay, are used in this study. Realizations of each of these types are shown in Fig. 1. All networks are generated by initially selecting a number of randomly positioned points in a cubic domain of edge length *L*, which are then used as seeds for the Voronoi tessellation of the respective volume. To generate the Voronoi network, the edges of the polyhedra resulting from the tessellation [14, 15] are retained as fibers. The fibers result with random orientations in space and the bulk coordination number is $z = 4$. Diluted Voronoi networks are generated from the Voronoi networks by eliminating a fraction of the fibers, such that the mean coordination number in the bulk is reduced to $z = 3$. Delaunay networks are the duals of the Voronoi networks and have a much higher fiber density and connectivity (mean coordination number of 15).

The Voronoi networks considered are below the isostaticity limit in 3D. In all cases the cross-links are considered welded joints and transmit both forces and moments between the filaments they connect. The finite bending stiffness of filaments renders the network stable

despite the fact that the coordination number is smaller than the minimum value required by the Maxwell structural stability relation [16].

The number of points selected in the respective volume defines the network density. The non-dimensional group ρA is used here in place of the density, ρ. Parameter ρA is also the volume fraction occupied by the network in the L^3 volume of the model.

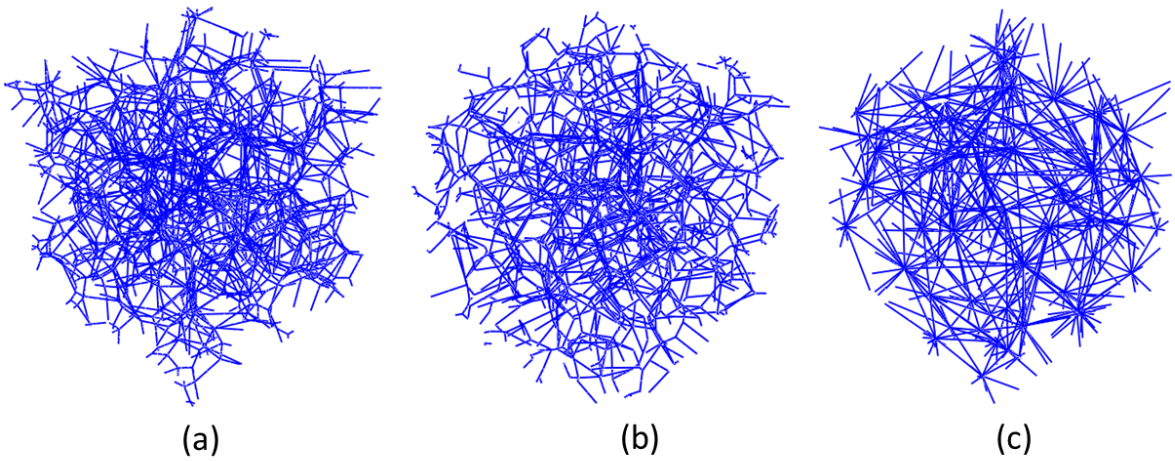

Figure 1. Realizations of the three types of three-dimensional networks considered: (a) Voronoi, (b) diluted Voronoi, and (c) Delaunay.

The fiber cross-section is defined by the area, *A*, and two principal moments of inertia, I_{min} and I_{max}. The principal directions of inertia are taken to be randomly oriented in the plane perpendicular to the fiber axis and uncorrelated with the fiber axis direction and from fiber to fiber. All fibers in the model are of the same type. We do not focus here on the effect of fiber crimp (discussed in a number of other works [e.g. 6,17,18]) and hence all fibers are considered straight in the undeformed configuration.

Table 1 shows the parameters of all Voronoi networks considered in this work. These include the normalized density, ρA and ranges for the two values of the bending length, $l_{b\,min} = \sqrt{E_f I_{min}/E_f A}$ and $l_{b\,max} = \sqrt{E_f I_{max}/E_f A}$. The range of the corresponding values of $I_{min}/I_{max} = (l_{b\,min}/l_{b\,max})^2$ are also listed for reference. For each situation, cases with very small torsional stiffness $G_f J \ll E_f I_{min}$, and large torsional stiffness, $G_f J \gg E_f I_{max}$, are considered as

limit situations. For beams with rectangular section of edge lengths b and h, with $b > h$, $l_{b\,min} = h/2\sqrt{3}$, $l_{b\,max} = b/2\sqrt{3}$, $I_{min}/I_{max} = (h/b)^2$ and $G_f J/E_f I_{min} = 12G_f\beta(b/h)/E_f$, where $\beta(b/h)$ depends weakly on b/h as the variable increases from 1 to 10 [19], which is the range of cross-section aspect ratios of practical interest. Such cases are also included in Table 1. Table 2 shows the parameters of the diluted Voronoi and Delaunay networks studied.

Table 1. Parameters of Voronoi networks considered in this study.

Regime	ρA	$l_{b\,min}/\sqrt{A}$	$l_{b\,max}/\sqrt{A}$	I_{min}/I_{max}
Bending dominated	3.29 10^{-4} to 1.65 10^{6}	5.77 10^{-7} to 0.0913	5.77 10^{-7} to 5.4	0.00286 to 1
Transition	32.9 to 9.88 10^{4}	3.04 10^{-4} to 0.913	3.04 10^{-4} to 0.913	0.0025 to 1
Axially dominated	3.29 10^{-4} to 32.9	0.04 to 2.49 10^{4}	0.913 to 5.4 10^{4}	0.002 to 1
Rectangular1	3.66 10^{-5} to 7.32 10^{-4}	0.0645 to 0.289	0.289 to 1.29	0.0025 to 1
Rectangular2	3.66 10^{-3} to 7.32 10^{-2}	0.0645 to 0.289	0.289 to 1.29	0.0025 to 1

Table 2. Parameters of diluted Voronoi and Delaunay networks considered in this study

Network	ρA	$l_{b\,min}/\sqrt{A}$	$l_{b\,max}/\sqrt{A}$	I_{min}/I_{max}
Diluted Voronoi	4.98 10^{-6} to 0.050	0.0645 to 0.289	0.282 to 1.291	0.0025 to 1
Delaunay	3.22 10^{-7} to 6.44 10^{-6}	0.0645 to 0.289	0.289 to 1.291	0.0025 to 1

Fibers are modeled using Timoshenko beams of generalized cross-section. The energy of the structure is computed by summing up the axial, bending and torsional strain energies of all filaments as described in [8]. The boundary conditions applied mimic uniaxial tension. Two opposite faces of the model are displaced relative to each other by specifying displacements in the loading direction. The other degrees of freedom of the same nodes are left free. The lateral faces are constrained to remain planar, but are free to move in the direction of their normal, therefore allowing for Poisson contraction. The rotational degrees of freedom of all boundary nodes are kept free. The model is solved using the finite element solver ABAQUS Implicit when only small strains are applied and ABAQUS Explicit for the large strains regime.

3. Results

Consider first the linear elastic deformation of the network subjected to small strains. The elastic modulus E is a function of all parameters listed in Tables 1 and 2 and a broad range of values results for all these systems. In line with the previous literature [e.g. 5,8], the data was collapsed on a master curve by properly selecting relevant non-dimensional groups. We discuss first the results for Voronoi networks. These are grouped in two categories: (i) systems with small torsional fiber stiffness, $G_f J \ll E_f I_{min}$, and (ii) systems with large fiber torsional stiffness, $G_f J \gg E_f I_{max}$. For each of these categories, all entries in Table 1 (over 150 systems) have been considered, with small and large values for $G_f J$ in cases (i) and (ii), respectively.

Figure 2 shows the collapsed data for the first category, (i), i.e. systems in which fiber torsion requires little energy compared with the energy stored in the other deformation modes. The vertical axis shows the network modulus, E, normalized with $\alpha(\rho A)E_f$, where α is a non-dimensional parameter of order unity which depends weakly on the network architecture. The same value of α is used for all data corresponding to given network type. Three non-dimensional groups are used on the horizontal axis, i.e. ρA, $l_{b\,min}/\sqrt{A}$ and $l_{b\,max}/\sqrt{A}$. The data collapses onto a master curve once the variable on the horizontal axis is selected as $w = \rho A \left(l_{b\,min}/\sqrt{A}\right)^{x}\left(l_{b\,max}/\sqrt{A}\right)^{2-x} = \rho\,(l_{b\,min})^{x}(l_{b\,max})^{2-x}$, with $x = 1.3$.

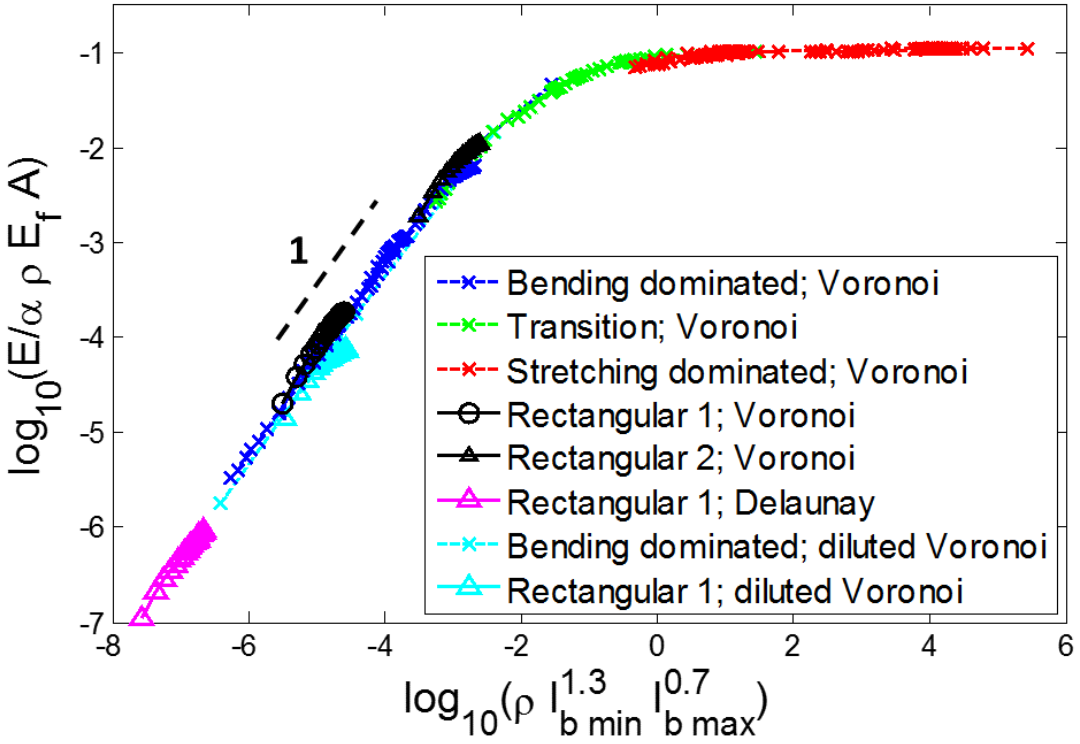

Figure 2. Master curve for the small strain network modulus, *E*, for Voronoi, diluted Voronoi and Delaunay systems with fibers having small torsional stiffness, $G_f J \ll E_f I_{min}$, case (i).

The curve is similar to that obtained for networks of fibers with circular section, i.e. indicates that for large densities and when both characteristic lengths $l_{b\,min}$ and $l_{b\,max}$ are large, the network modulus is proportional to $(\rho A)E_f$. In this regime the deformation is largely affine. For small values of *w*, the curve has slope 1 and $E \sim \rho^2$, which is similar to the results reported for 3D open cell foams [13], and $E \sim E_f I_{min}(I_{max}/I_{min})^{1-x/2}$. In this regime the deformation is non-affine.

As in the case of networks of fibers with circular section, the dominant deformation mode in the non-affine regime is bending. If all fibers would be free to rotate such to deform in the softest bending mode, one would expect $E \sim E_f I_{min}$. The correction term $(I_{max}/I_{min})^{1-x/2} = (I_{max}/I_{min})^{0.35}$ represents the effect of the constraint imposed by the structure on fiber twist, which prevents full rotation and bending in the softest mode.

In order to test the generality of these conclusions, we perform a similar analysis with Delaunay and with diluted Voronoi networks of mean coordination $z = 3$. The results are shown in Fig. 2 and include the reference case of fibers with circular cross-section, as well as all cases of fibers with non-circular section listed in Table 2. The data collapse on the same master curve indicating similar behavior of these network architectures. We used α = 1 for the Voronoi network, α = 0.52 for the diluted Voronoi and α = 0.27 for the Delaunay networks. The same value of α is used for all networks of given type, including for those of fibers with circular cross-section.

To further evaluate the effect of the torsional stiffness of fibers on exponent *x*, Voronoi networks with $G_f J \gg E_f I_{max}$ and with the various parameter sets listed in Table 1 are considered, case (ii). In this situation the energy cost associated with filament twist should force bending in both hard and soft modes, as dictated by the local geometry and initial configuration. The results for these models are presented in Fig. 3. In this case, it is observed that data collapse results for $x = 1$, which indicates that both bending modes contribute equally to the mechanics of the network.

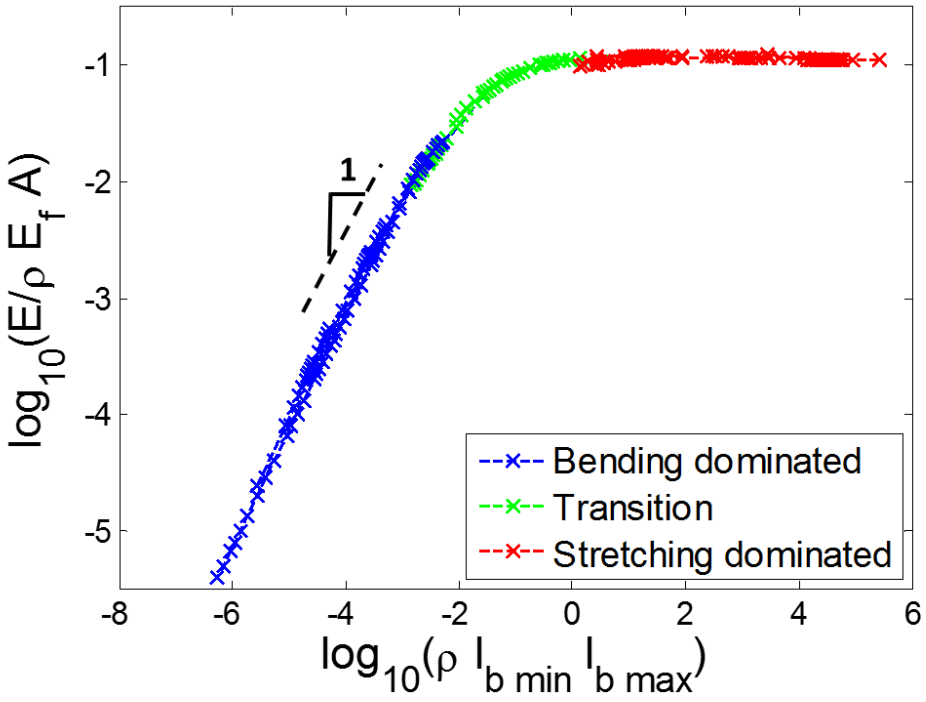

Figure 3. Master curve for network modulus, E, for Voronoi networks of fibers with large torsional stiffness, $G_f J \gg E_f I_{max}$, case (ii). Parameter α used in Fig. 2 is equal to 1 for Voronoi networks.

Further, we verify that the effect of the torsional stiffness of filaments is restricted to that described above, i.e. it controls the relative contribution of the two bending modes to the network elasticity. To this end, Voronoi networks with $I_{max} = I_{min}$ are considered and *J* is varied independently in a broad range. This situation appears inconsistent with the behavior of beams, but may apply to molecular filaments and serves the purpose of testing the stated conjecture. No *J*-dominated regime of the network elasticity emerges, even for very small values of the torsional stiffness. This result is not new. However, it is useful to compare it with the situation in which the shear stiffness $G_f A$ is artificially reduced, case in which a shear dominated regime appears and the network modulus becomes proportional to $G_f A$ [20]. This limit case has only a theoretical importance since this type of deformation may take place only in beams (not in molecular filaments), but the range of parameters for which the shear mode dominates is unreachable in practical applications, for beams of realistic cross-sections.

Further, it is interesting to inquire to what extent the behavior described above for the small strain modulus extends to large deformations. To investigate this issue, multiple Voronoi networks of fibers with rectangular cross-section and a broad range of cross-sectional aspect ratios $h/b = \sqrt{l_{b\,min}/l_{b\,max}}$, $1/40 < h/b < 1$, are considered. All these configurations correspond to the same value of parameter *w*, $(w = log_{10}(\rho\, l_{b\,min}^{1.3} l_{b\,max}^{0.7}) = -4.45$, which places them in the bending-dominated, non-affine range, all belong to type (i) discussed above and have the same value of ratio $G_f J / E_f I_{min} \sim 1/12$. Therefore, all networks used for this purpose have the same small strain modulus.

These networks are deformed uniaxially into the strain stiffening range of strains. Figure 4 shows the tangent stiffness-stress plot for systems with h/b = 1, 1/10, 1/20 and 1/40. It is seen that the curves overlap in both the small strain (which is expected since all these systems have same value of *w*) and the large deformations regimes. As previously observed for this type of networks [21,22], the large strain branch of the stress-strain curve is exponential and hence the

tangent stiffness varies linearly with the stress. The data in Fig. 4 indicate that the aspect ratio of the cross-section, h/b, has no effect on the large strain behavior.

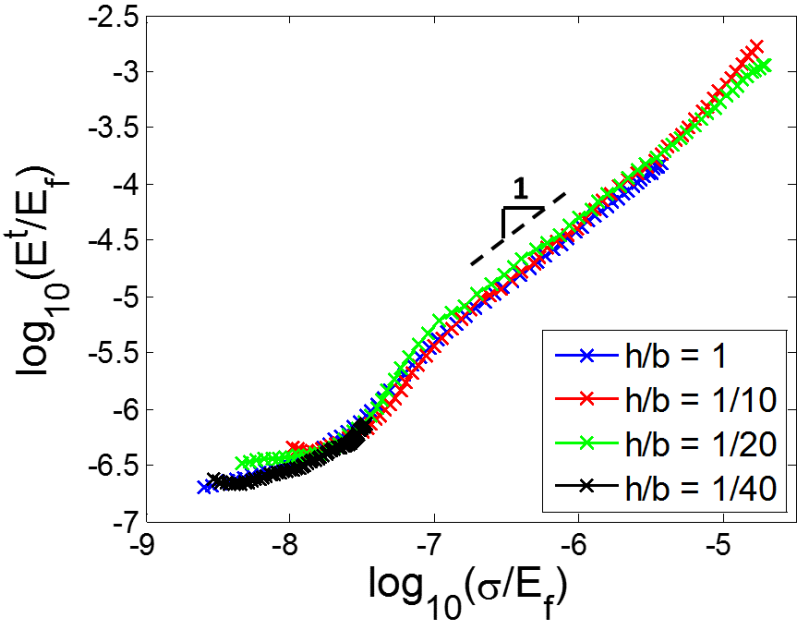

Figure 4. Tangent stiffness ($E^t = \partial\sigma/\partial\varepsilon$) for Voronoi networks of fibers with different cross-sections. The cross-section aspect ratio, *h/b*, varies from 1/40 to 1.

4. Conclusions

In this work we consider random fiber networks of three different architectures, composed from fibers having cross-sections characterized by two unequal principal moments of inertia. Such fibers may deform either axially or in two, hard and soft, bending modes. We investigate the effect of the presence of two bending modes on the small and large strain network behavior. The small strain modulus is described in terms of the network parameters through a master plot similar to that previously discussed in the literature for random networks of fibers with circular cross-section. The exponents leading to data collapse depend on the torsional stiffness of the filaments. If this parameter is small, fibers tend to rotate such to allow deformation in the soft bending mode, which increases the importance of $l_{b\,min}$. If torsional stiffness is large, fibers bend with equal probability in the soft and hard bending modes and

hence $l_{b\,min}$ and $l_{b\,max}$ are equally important. This observation holds for all three architectures studied. The large deformation behavior is controlled by the transition from the bending to the axial deformation modes and hence the distinction between the soft and hard bending modes has little effect at large strains.

Acknowledgment

We gratefully acknowledge the financial support of the National Institute of Health (Grant Nos. RO1-EB005813 and U01-EB016638).

References

1. P. Kannus, Scand. J. Med. Sci. Sports **10**, 6 (2000).
2. J. W. S. Hearle, P. Grosberg, and S. Backer, *Structural Mechanics of Fiber Yarn and Fabrics* (Wiley, 1969).
3. M. W. D. Van der Burg, V. Shulmeister, E. van der Geissen, and R. Marissen, J. Cell. Plast. **33**, 1 (1997).
4. T. Komori, K. Makishima, Tex. Res. J. **47**, 13 (1977).
5. D. A. Head, A. J. Levine, and F. C. Mackintosh, Phys. Rev. E **68**, 6 (2003).
6. P. R. Onck, T. Koeman, T. Van Dillen, and E. Van der Giessen, Phys. Rev. Lett. **95**, 17 (2005).
7. J. Wilhelm, and E. Frey, Phys. Rev. Lett. **91**, 10 (2003).
8. A. S. Shahsavari and R. C. Picu, Int. J. Solids Struct. **50**, 20 (2013).
9. G. Subramanian and R. C. Picu, Phys. Rev. E **83**, 5 (2011).
10. E. Ban, V. H. Barocas, M. S. Shephard, and R. C. Picu, J. Mech. Phys. Solids **87**, (2016).
11. E. L. G. Wernersson, B. Svetlana, A. Kulachenko, and G. Borgefors, Nord. Pulp. Res. J. **29**, 3 (2014).
12. W. E. Warren and A. M. Kraynik, J. Appl. Mech. Tran. ASME **55**, 2 (1988).

13. L. J. Gibson and M. F. Ashby, *Cellular solids: structure and properties* (Cambridge university press, 1999).
14. W. Y. Jang, A. M. Kraynik, and S. Kyriakides, Int. J. Solids Struct. **45**, 7 (2008).
15. D. F. Watson, Comput. J. **24**, 7 (2008).
16. C. R. Calladine, Int. J. Solids Struct. **14**, 2 (1978).
17. E. Ban, V. H. Barocas, M. S. Shephard, and R. C. Picu, J. Appl. Mech. Tran. ASME **83**, 4 (2016).
18. A. Kabla and L. Mahadevan, J. R. Soc. Interface **4**, 12 (2007).
19. A. C. Ugural and S. K. Fenster, *Advanced strength and applied elasticity* (Elsevier Publishing Company, 1981).
20. E. Ban, *Effective properties of random composites and fiber networks*, PhD Thesis, Rensselaer Polytechnic Institute, 2015.
21. A. J. Licup, S. Münster, A. Sharma, M. Sheinman, L. M. Jawerth, B. Fabry, D. A. Weitz, and F. C. MacKintosh, Proc. Natl. Acad. Sci. U.S.A. **112**, 31 (2015).
22. G. Zagar, P. R. Onck, and E. Van der Giessen, Macromolecules **44**, 17 (2011).